

Free energy changes on freezing and melting ductile metals

By R. M. LYNDEN-BELL

University Chemical Laboratory, Lensfield Road, Cambridge CB2 1EW, England

J. S. VAN DUIJNEVELDT

Van't Hoff Laboratory, University of Utrecht, Padualaan 8, 3584 CH Utrecht,
The Netherlands

and D. FRENKEL

FOM Institute for Atomic and Molecular Physics, Kruislaan 407,
1098 SJ Amsterdam, The Netherlands

(Received 26 March 1993; accepted 26 April 1993)

The variation in Landau free energy while melting platinum was investigated at a number of temperatures using computer simulation with a model potential. The technique used was to apply a biasing potential in a Monte Carlo simulation with umbrella sampling. From the Landau free energy curves one can determine the difference in free energies between the solid and liquid phases easily and accurately, the thermodynamic melting point (T_m), and the limit of metastability of the crystalline phase. The latter occurs at approximately $1.2T_m$. It was difficult to freeze the material, but, using a suitable order parameter, this was achieved. Unlike earlier results on a soft sphere system, there was no evidence for nucleation of a metastable body-centred-cubic phase. One possible reason is the existence of local icosahedral order in the liquid phase of the metal. The surface free energy of the solid-liquid surface was estimated from the free energy barrier to melting. Model rhodium behaved in a very similar way.

1. Introduction

The phase transition between a solid and a liquid is a first-order phase transition. As there is a free energy barrier between the phases, it is necessary to nucleate the new phase within the old phase and thermodynamic equilibrium may be slow to be established. In real systems it is easy to supercool liquids and in simulations both supercooling of liquids and superheating of solids occur all too easily. The reason for this is that most simulations of bulk material use periodic boundaries and so have no surfaces at which melting can be initiated, and the small size of the system makes it very improbable that defects within the crystalline phase are present. As a result, the observed melting point in a standard bulk simulation in which the temperature of a perfect crystal is slowly raised is the limit of metastability of a perfect crystal rather than its thermodynamic melting point. Yip and coworkers [1, 2] have termed this the limit of mechanical stability.

On cooling (with care) both real systems and simulated systems can be supercooled eventually forming glasses. The more stable crystalline phase can only form by nucleation. The process of nucleation is of considerable interest and has been

studied both theoretically and experimentally for many years. However the time scales involved make direct computer simulation of freezing and melting of atomistic models expensive [3]. Recently Frenkel and van Duijneveldt [4] introduced a new method for studying the process using a biased Monte Carlo (MC) method with umbrella sampling. Essentially in this method a fictitious field is applied to the system which interacts with a suitable order parameter to force the system to freeze or melt. The free energy in the presence of the field is measured and the free energy in the absence of the field is then determined by subtracting the interaction term.

van Duijneveldt and Frenkel applied this method to a system of soft spheres and showed that, although the stable solid state of this system is known to be face-centred-cubic (f.c.c.) at 0 K and thought to be f.c.c. up to the melting point, no smooth path for the melting or freezing transition between liquid and solid was found. Instead as the f.c.c. solid is forced to disorder at a temperature near the melting point it makes a discontinuous change, while when the melt is forced to order a body-centred-cubic (b.c.c.) phase with defects is formed in preference to the expected f.c.c. phase.

In this paper we extend the work to materials with a very different intermolecular potential, namely two pairs of metals, platinum/gold and silver/rhodium. Platinum was chosen because it is particularly ductile compared to a soft sphere or to a Lennard-Jones solid. A measure of this is given by the ratio of the shear elastic constant c_{44} to the bulk compressibility B . Values are given in table 1, which show that platinum and gold, in particular, have a very low value of this parameter suggesting that atoms in these metals can move easily relative to each other, and so may be able to melt and freeze more smoothly.

We do indeed find different behaviour for the metals and the soft-sphere system. Platinum can be forced to disorder at the melting point smoothly and reproducibly. Freezing is a more difficult process. By using an order parameter that biases configurations towards a f.c.c. structure we do obtain smooth freezing, and the curve of free energy as a function of order parameter on freezing is very close to that for melting. Using a less biased order parameter kinetic considerations seemed to prevent freezing on the time-scale available.

We also investigate the effects of temperature on the melting process and show that the free energy barrier to melting decreases until the limit of stability of the solid phase is reached. This free energy barrier is related to the surface free energy between the solid and liquid phases and we give estimates of this surface free energy.

Finally we present some results on the degree of local order in the liquids.

Table 1. Some properties of argon and the metals that are modelled.

	Argon	Pt	Au	Ag	Rh
Model	Lennard-Jones	S-C 10,8	S-C 10,8	S-C 12,6	S-C 12,6
Length/ \AA ^(a)	5.3	3.92	4.08	3.80	4.09
Energy/ $k_B K$ ^(b)	930	67800	43760	65500	33720
c_{44}/B (model)	0.80	0.27	0.27	0.53	0.53
c_{44}/B (expt)	0.62	0.27	0.27	0.47	0.72
T_m/K (model)		1400	905	2200	1150
T_m/K (expt)		2042	1338	2236	1235

^(a) Lattice constant at 0 K. Values for Lennard-Jones system from [18] and for the Sutton-Chen potentials from [5].

^(b) Binding energy at 0 K; references as above.

2. Method, potentials and order parameters

In order to model a metal it is necessary to use an interatomic potential with many-body character rather than one which is the sum of pair terms. For this work we use the semi-empirical potentials developed by Sutton and Chen [5], which are of the type proposed by Finnis and Sinclair [6] with the form

$$U = \sum_{ij} U(r_{ij}) - \sum_i u(\rho_i)^{1/2}. \quad (1)$$

The first term represents the repulsion between atomic cores and the second term models the bonding energy due to the electrons. The local density, ρ_i , in the second term is the local density of atoms. In Sutton and Chen's potentials this is given by

$$\rho_i = \sum_j \left(\frac{a}{r_{ij}} \right)^m, \quad (2)$$

and the pair repulsion is also modelled by a reciprocal power so that the complete potential is

$$U = \epsilon \left\{ \sum_{ij} \left(\frac{a}{r_{ij}} \right)^n - C \sum_i \left[\sum_j \left(\frac{a}{r_{ij}} \right)^m \right]^{1/2} \right\}. \quad (3)$$

This represents a family of potentials whose members differ in the exponents (n and m). Once these are fixed all other properties are related by scaling. Only two of the three parameters ϵ , C and a , are independent, and all are completely determined by the equilibrium lattice parameters and lattice energy of the face-centred lattice at 0 K. Sutton and Chen assigned exponent pairs (n, m) for modelling different metals by fitting the elastic constants as closely as possible. The ratio of the bulk elastic constant to the cohesive energy per unit volume is proportional to the product of the exponents, while the ratio of the shear to the bulk elastic constant depends mainly on the difference of the exponents. Sutton and Chen [5] give parameters for ten f.c.c. metals. Here we use only two of the Sutton-Chen family, the (10, 8) potential which models platinum and gold, and the (12, 6) potential which models silver and rhodium. Parameters are given in table 1. The former is very soft, while the latter is less so (see table 1). For computational convenience a cut-off was used so that atoms further apart than 2.1 times the nearest neighbour distance did not contribute to the potential.

2.1. Landau free energy

The main results of this work are the curves of free energy as a function of order parameter (see figures 1–5). These were constructed using an umbrella sampling method as described in [4]. The free energy that is shown in these figures is the Landau free energy. It is a function of some order parameter, Q , and is defined by

$$F(Q_0) = -kT \log \int \exp[-\beta(H_0 + p_{\text{ext}}V)] \delta(Q - Q_0) d\tau, \quad (4)$$

where the integral is over all phase space and p_{ext} is a constant equal to the external pressure. It is directly related to the probability $P(Q_0) dQ$ that the system has a value

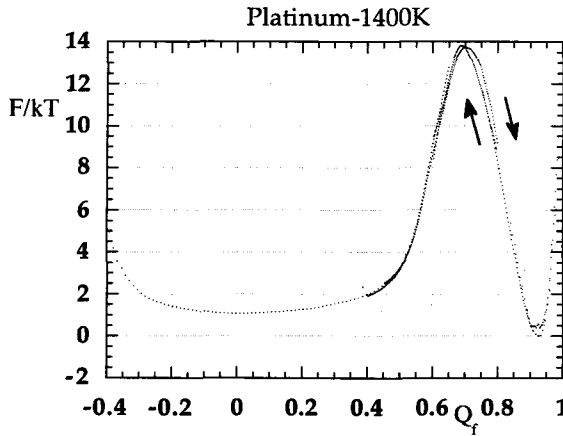


Figure 1. Landau free energy as a function of the order parameter Q_f for melting and freezing a lattice of 128 atoms of platinum at 1400 K. The left hand well corresponds to the liquid and the right hand well to the solid.

of the order parameter between Q_0 and $Q_0 + dQ$ which is given by

$$P(Q_0) = \int \exp[-\beta(H_0 + p_{\text{ext}}V)]\delta(Q - Q_0) d\tau / Z(p_{\text{ext}}), \tag{5}$$

by

$$F(Q_0) = -kT \log P(Q_0) + G(p_{\text{ext}}), \tag{6}$$

and, as the relative probabilities can be measured in the simulation, differences in the Landau free energy may be calculated. In these equations $Z(p_{\text{ext}})$ and $G(p_{\text{ext}})$ are constants whose values depend on the pressure.

In order to calculate changes in $F(Q)$ we calculate the relative probabilities of finding different values of Q in a constant temperature, constant pressure ensemble using a MC program with umbrella sampling to improve the statistics [7]. The probability of different values of Q within a certain range is constructed using a Hamiltonian $H_W = H_0 + W(Q)$ where $W(Q)$ is a function of Q chosen to try to equalize the probabilities of different values of Q . If $p_W(Q)$ is the probability calculated using the Hamiltonian H_W , then the required free energy corresponding to the true Hamiltonian H_0 is given by

$$F(Q) = -kT \log [p_W(Q)] - W(Q) + G. \tag{7}$$

For maximum efficiency in the sampling $W(Q)$ should be as close to $-F(Q)$ as possible. In practice we take a small window of Q values, find $F(Q)$ and construct $W(Q)$ for the next window by extrapolating $F(Q)$. The starting configuration for one window is chosen from a configuration from the previous window with an extreme value of Q . The MC program was adapted from that used by van Duijneveldt and Frenkel [4], and the fitting program was identical.

The runs were carried out using truncated octahedral boundary conditions. These have the advantage that the MC cell is fairly spherical and should not unduly influence the structure of the solid formed on freezing, but suffer from the disadvantage that the initial ideal f.c.c. lattice of the metals is only consistent with the b.c.c. structure of the MC calculation (b.c.c. because of the form of the boundary conditions) if the number of particles is $16 \times (n)^3$. The second smallest size is 128

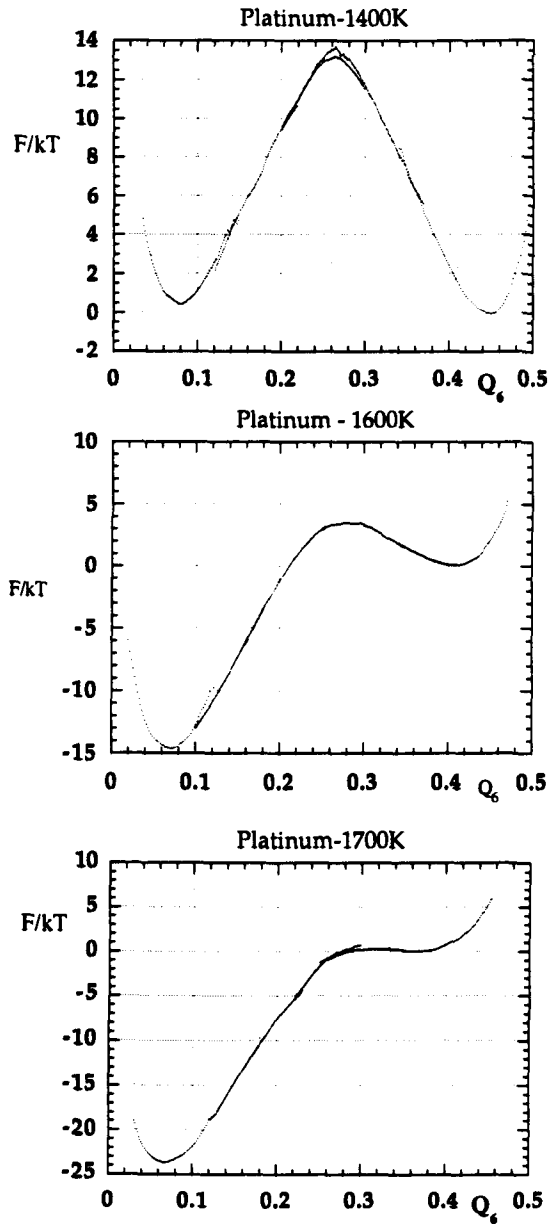


Figure 2. Landau free energy as a function of Q_6 for melting a lattice of 128 atoms of platinum at 1400 K, 1600 K and 1700 K. The left hand wells correspond to the liquid and the right hand wells to the solid.

particles, and most calculations were carried out for this number. However it is rather too small for comfort and a few calculations were carried out for the second next size, 1024 particles, which were much slower. Not only are there more particles to interact with each other, but also the windows in order parameter have to be smaller to avoid overflow in the weighting function. Each series was initiated from a solid made from an ideal f.c.c. lattice equilibrated at the required temperature, or

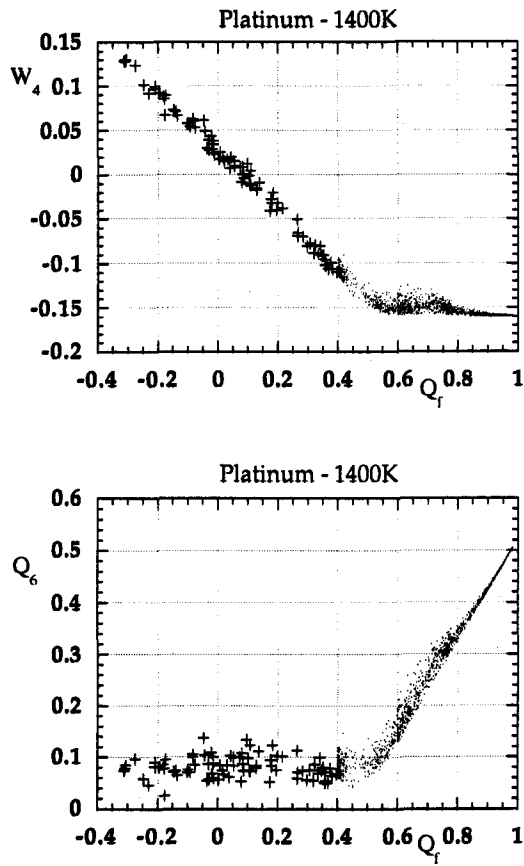


Figure 3. Variation of the order parameters W_4 and Q_6 as a function of Q_f for freezing platinum at 1400 K. The points marked with crosses are from the unbiased liquid, while the other points show the variation during freezing.

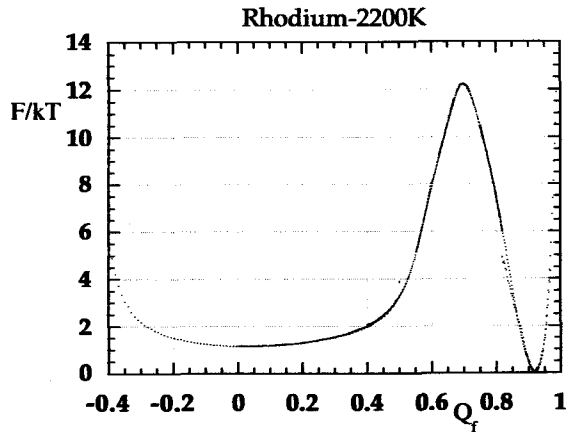


Figure 4. Landau free energy as a function of Q_f for melting a lattice of 128 atoms or rhodium at 2200 K. The left hand well corresponds to the liquid and the right hand well to the solid.

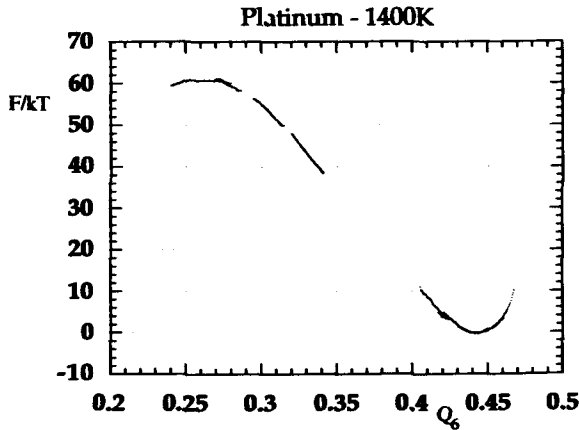


Figure 5. Landau free energy as a function of Q_6 for melting a lattice of 1024 atoms of platinum at 1400 K. The well corresponds to the solid phase.

from a solid at a different temperature, or from a liquid at a different temperature. Individual windows in the small system sizes were explored with runs of 50–80 K complete MC cycles (1 cycle corresponds to attempted moves of 128 particles chosen at random, followed by an attempted change of box size). The displacements were chosen to give approximately 50% chance of acceptance.

2.2. Free energy and equilibrium

$F(Q)$ is the basic concept in the Landau theory of continuous phase transitions [8], and can also be used to discuss first-order phase transitions. If $F(Q)$ has a single minimum (or well), then there is a single stable phase with the corresponding value of Q . If there are two wells then there are two possible phases. At the thermodynamic phase transition point the probabilities of finding a system from the ensemble in each well are equal, while the limit of metastability of the less stable phase occurs when the second minimum disappears. The life-time of the metastable phase depends on the height of the free energy barrier between the two minima, and can be very long if this is much greater than kT .

The relative values of the Gibbs free energies of two phases corresponding to different minima in the Landau free energy curves can be found from the Landau free energy curves. The Gibbs free energy of a phase, l , is given by

$$G_l = -kT \log \int_l \exp[-\beta(H_0 + p_{\text{ext}}V)] d\tau, \quad (8)$$

where the integral is taken over that part of phase space which corresponds to the phase l . The difference in the Gibbs free energy of the liquid and crystalline phases is related to the probabilities P_l and P_c of finding the system in the liquid and crystal well respectively by

$$G_l - G_c = -kT \log (P_l/P_c). \quad (9)$$

As the probability that the system has an order parameter between Q and $Q + dQ$ is

given by equation (5), we have (using equation (6))

$$P_l = \int_l P(Q) dQ$$

$$= Z^{-1} \int_l \exp[-\beta F(Q)] dQ, \quad (10)$$

where Z is a normalisation constant which ensures that $P_l + P_c = 1$. Near each energy minimum one may perform a Taylor expansion

$$F(Q) = F_{\min} + (Q - Q_{\min})^2 / (2\sigma^2) \dots \quad (11)$$

As the system size increases, the minima become sharper and the probability distribution in each well becomes Gaussian with width σ

$$P_l = Z^{-1} \exp(-\beta F_{l,\min}) \int_l \exp\left[-\frac{\beta(Q - Q_{l,\min})^2}{2\sigma^2}\right] dQ. \quad (12)$$

Using the standard expression for the integral of a Gaussian function we obtain

$$P_l = (2\pi)^{1/2} \sigma_l Z^{-1} \exp(-\beta F_{l,\min}). \quad (13)$$

Hence the difference between the Gibbs free energies of the two phases is

$$G_l - G_c = F(Q_{l,\min}) - F(Q_{x,\min}) - kT \log(\sigma_l / \sigma_c), \quad (14)$$

where $F(Q_{x,\min})$ and $F(Q_{l,\min})$ are the values of the Landau free energy at the bottom of the two wells. Unless the curvatures are very different, the second term in equation (14) is a small correction and the condition for coexistence is essentially that the minima in the Landau free energies are equal.

In our simulations the curvatures of the two wells in the Landau free energy expressed as a function of Q_6 were very similar, so that to a good approximation, the relative stability of the bulk phases in the thermodynamic limit is given by the relative position of the free energy minima in the Landau free energy expressed as a function of Q_6 . The difference in values of the Landau free energy at the minima could be found quite accurately.

2.3. Order parameters

In their analysis, van Duijneveldt and Frenkel used four collective order parameters, Q_4 , Q_6 , \hat{W}_4 and \hat{W}_6 based on the bond order parameters introduced by earlier workers [9]. In order to construct these, bonds are drawn between all atoms nearer than a prescribed cut-off distance (we used 1.24 times the nearest neighbour separation). The Q_L order parameter is made up of sums of spherical harmonics for all N_b bonds in the system

$$Q_L^2 = \frac{4\pi}{N_b^2(2L+1)} \sum_m \left| \sum_{bonds} Y_{L,m}(\hat{r}_{ij}) \right|^2, \quad (15)$$

and are invariant under rotations, while the \hat{W}_L functions are the third-order invariants

$$\hat{W}_L = \sum_{m_1, m_2} \begin{pmatrix} L & L & L \\ -m_1 & -m_2 & m_1 + m_2 \end{pmatrix} \bar{Q}_{L,-m_1} \bar{Q}_{L,-m_2} \bar{Q}_{L,m_1+m_2}, \quad (16)$$

where

$$\bar{Q}_{L,m} = \frac{\sum_{bonds} Y_{L,m}(\hat{r}_{ij})}{(\sum_m |\sum_{bonds} Q_{L,m}(\hat{r}_{ij})|^2)^{1/2}}. \quad (17)$$

Table 2 (taken from [4]) shows how these order parameters vary for different ideal space filling lattices (f.c.c., b.c.c., hexagonal closest packed (h.c.p.) and simple cubic). The order parameter Q_6 has a similar value for all four ideal lattices, while an order parameter Q_f defined by

$$Q_f = Q_6 - 3W_4 \quad (18)$$

selects the f.c.c. structure rather than h.c.p., b.c.c. or simple cubic. In the rest of the paper we write W for \hat{W} to simplify the notation.

Local order parameters can be defined in a similar way to the global ones, with only the spherical harmonics of the bonds around each atom being averaged before squaring. The values for the local order parameters in the space-filling-lattices are the same as the values for the global order parameters. The entry in the table for icosahedral order can only be used to describe the local order around an atom at the centre of a regular icosahedral structure, as icosahedra are not space filling.

3. Results

3.1. Melting and freezing at the thermodynamic melting temperature

Figures 1 and 2 show curves of $F(Q)/kT$ for platinum at 1400 K calculated for the two different order parameters, Q_f and Q_6 . This temperature was chosen as previous work on the melting at surfaces [10] showed that the thermodynamic melting point was between 1400 K and 1450 K. In the first series of runs (figure 2(a)) the system melted smoothly as the biasing potential $W(Q)$ was changed to force Q_6 to decrease. The whole process could be monitored using five or six windows of Q_6 . At this temperature it appears from figure 2 that the free energy minimum of the solid is $0.5kT \pm 0.5kT$ more stable than the minimum free energy of the liquid. The magnitude of the free energy barrier to melting is $(13.5 \pm 1)kT$. The ordinate of this graph is the free energy of the whole system measured in units of kT . At 1400 K one unit is equal to $11.64 \text{ kJ mol}^{-1}$ for the whole system of 128 particles or $0.091 \text{ kJ mol}^{-1}$ per atom in the system, so that the relative free energy of the two states is determined to about 0.05 kJ mol^{-1} .

When one tries to reverse the process, starting from the liquid and increasing Q_6 difficulties arise. No second minimum was found in spite of several runs in a window of Q_6 near the observed maximum in the melting process. The free energy apparently

Table 2. Order parameters in ideal configurations.

	Q_4	Q_6	W_4	W_6	Q_f
f.c.c.	0.191	0.575	-0.159	-0.013	1.052
h.c.p.	0.097	0.485	0.134	-0.012	0.082
b.c.c.	0.036	0.511	0.159	0.013	0.033
Simple cubic	0.764	0.354	0.159	0.013	-0.124
Icosahedral (local)	0	0.6632	0	-0.170	0.6632

increased monotonically as Q_6 was forced to increase, reaching values well above the free energy barrier for melting found in the melting run (figure 1). We attribute the lack of freezing to kinetic effects, and examination of configurations showed the problem. In order to obtain an f.c.c. lattice it is necessary for the third-order invariant W_4 to be negative. In the freezing runs the values of W_4 in configurations in which Q_6 was increasing were positive, and did not fluctuate into the negative region. In order to confirm that melting and freezing process are reversible a run was done using the order parameter Q_f which biases the system towards the f.c.c. structure. Figure 1 shows the free energy changes during two runs in which a solid configuration was melted and a liquid configuration was frozen. The melting and freezing curves agree well. The liquid corresponds to a very wide range in values of Q_f . Figure 3 shows the variation of the order parameters as a function of Q_f , from which it will be seen that *in the liquid* W_4 and Q_f are strongly correlated, while Q_6 is less so. As the value of Q_f is forced to increase towards the barrier W_4 remains negative and Q_6 starts to increase. Thus the use of Q_f as an order parameter aids the freezing process by favouring configurations from the liquid with negative values of W_4 , while using Q_6 does not seem to favour these configurations. Although it seems to be difficult for the system to find the transition state to the solid, there is no evidence for freezing to some other structure with a lower free energy barrier, unlike the behaviour in the soft sphere system [4] which seemed to favour a disordered b.c.c. phase.

The fact that the free energy barriers in the freezing and melting runs using Q_f are equal to each other, and equal to the barrier measured in the melting runs using Q_6 , gives one confidence that these barriers are reproducible to an accuracy of about kT (0.1 kJ mol^{-1}). The minimum in the liquid well is about $1kT$ above the minimum in the solid well, which is greater than the minimum shown in figure 2 calculated using Q_6 . This is to be expected as the liquid well is broader. The arguments given in section 2.1. show that, if the probability of being in two wells of different curvature is the same, the minimum of the broader well must be higher than the minimum of the narrower well.

3.2. *Temperature dependence of the free energy changes*

Figure 2 shows the curves of free energy as a function of Q_6 for the platinum potential at three different temperatures, 1400 K, 1600 K and 1700 K. The zero of free energy is fixed arbitrarily at the free energy of the crystal at that temperature. This method does not give absolute free energies, or the change of free energy between runs at different temperatures. These curves provide a striking demonstration of the difference between the thermodynamic melting point (just above 1400 K) and the limit of metastability of the solid (just above 1700 K). The free energy of the solid rises relative to the liquid as the temperature is increased, and at the same time the barrier from solid to liquid decreases. At 1700 K it has nearly gone and the limit of metastability is close to this temperature. This is in agreement with molecular dynamics simulations of the crystalline phase at constant pressure using periodic boundary conditions and 512 particles, where it was found that the crystal phase could be simulated up to about this temperature, but at 1800 K melting occurred spontaneously [11]. In such a simulation there are no defects or surfaces to initiate melting, so that the limit of metastability is found rather than the thermodynamic melting point.

3.3. Variation with potential

The difference in behaviour between soft spheres and platinum led us to explore the behaviour of the freezing of a less ductile metal, namely rhodium. This was modelled using a (12-6) Sutton–Chen potential with the parameters given in [5]. Surface melting studies [10] had suggested that this potential has a thermodynamic melting point near 2200 K. The melting curve for rhodium at 2200 K using the Q_f order parameter is shown in figure 4 and is practically identical to that for platinum shown in figure 1. Once again the solid is more stable than the liquid by about kT or 0.14 kJ mol^{-1} , giving a free energy barrier of $12.5kT$ or 230 kJ mol^{-1} for the system of 128 atoms. This is about 35% higher than the free energy barrier for platinum, although slightly lower as a multiple of the temperature. Although this potential is harder and the material more rigid, there was no difficulty in obtaining a smooth transition between solid and liquid, unlike the very short-ranged purely repulsive soft sphere potential investigated in [4].

3.4. Estimation of surface free energy

The potential barrier at coexistence depends on the value of the surface free energy of the boundary between the phases. As melting is induced, a small pool of liquid forms within the solid with a free energy cost due to the surface between liquid and solid (the free energies of the bulk phases are equal at coexistence). Thus

$$\Delta F = \gamma A, \quad (19)$$

where γ is the surface free energy per unit area and A is the area of the surface. There is also a small contribution due to the fact that the density of liquid and solid cannot adjust exactly to their equilibrium values although the average external pressure is kept constant (equal to zero in these simulations). As the order parameter decreases, the volume and surface area of the liquid increases. Eventually the system can lower its surface area by changing its geometry. Among the possibilities are, that it forms a series of parallel slabs of solid and liquid with surfaces parallel to one of the [110] planes, or an infinite cylinder parallel to one of the [111] directions, or a bicontinuous triply periodic phase similar to the ‘plumber’s nightmare’ [12]. Of these possibilities the least surface area corresponds to the parallel slabs ($A = 1.414b^2$), the surface area of a cylinder with half the total volume is equal to $A = 1.65b^2$, while that of the plumber’s nightmare is $A = 2.35b^2$. In these expressions, b is the length of the side of the cube that contains the truncated octahedron whose volume is $V = b^3/2$. The surface area of a sphere with half the volume of the MC cell is $A = 1.92b^2$.

Provided that the transition from the initial sphere to a continuous phase is smooth, the free energy barrier is equal to the product of the surface free energy per unit area of the liquid-crystal interface and the maximum surface area of the surface. This cannot be estimated accurately from the simulations on small samples as there are not enough atoms to form distinct solid and liquid phases with a well defined surface between them. Equally, very large systems would prove difficult to use, as the required change of geometry would not be smooth. Figure 5 shows the results from simulations of platinum with 1024 atoms. The transition appears to be smooth and examination of configurations suggests that there are cylinders of ordered material in the region of the maximum free energy.

The free energy barrier is $\Delta F = (60 \pm 5)kT = (1.2 \pm 0.1) \times 10^{-18} \text{ J}$. The width of the simulation box at the top of the free energy barrier is $b = 3.26 \times 10^{-9} \text{ m}$.

Combining these we get an estimate of the surface free energy between the crystal and the liquid phases at coexistence of 0.07 J m^{-2} . This estimate has a number of uncertainties, but is probably within 20% of the true answer.

The surface energy (not free energy) of the solid in contact with vapour at 0 K was measured by Todd and Lynden-Bell [10] as a function of temperature. At 0 K the surface energies of a (111) crystal surface in contact with vacuum is 0.9 J m^{-2} , while that for a more open (100) surface is 1.02 J m^{-2} . Although these values were found to increase with temperature, the surface free energies are expected to decrease due to the entropic contribution. At 1500 K the surface energy (not free energy) of the liquid in contact with vacuum was found to be 0.9 J m^{-2} [10]. In this work we are measuring the free energy of the solid-liquid boundary, and it is not surprising that we obtain a much smaller value than for the solid-vapour or liquid-vapour boundaries. In fact, the phenomenological Miedema model [13-15] predicts that the solid-liquid interfacial free energy is, typically, one order of magnitude smaller than the solid-vapour interfacial free energy. An experimental value for the surface free energy for the solid-liquid boundary in platinum has been estimated from nucleation studies [16] to be 0.24 J m^{-2} . Although our result is lower than the experimental value phase space of by a factor of three, we also found [10] that the surface energy of the solid-vapour surface is too low, and the material melts at a lower temperature than platinum does. The discrepancy between the estimate and the experiment is more likely to be a shortcoming of the model we use for platinum than a problem with the method.

3.5. Local and global order parameters

Table 3 shows the observed values of various order parameters in the solid and liquid states. These were measured in runs with no applied field or weighting, so they are typical of the liquid or solid.

The global order parameters for the liquid phase should tend to zero in the thermodynamic limit of large N . The change in these values between the run at 1400 K with 128 particles and the run at the same temperature with 1024 particles is in accord with this. The local order parameters for the large and small runs at 1400 K agree well, so that the results from runs on small systems at 1600 K and 1700 K should provide an accurate measure of the local order in the liquid at these temperatures. We may also conclude that the 128 particle simulations give reasonably accurate descriptions of the homogeneous bulk phases.

Table 3. Observed values of local order parameters in the simulations.

	Sol Pt	Liq Pt	Liq Pt	Liq Pt	Liq Pt	Sol Rh	Liq Rh
T	1400 K	1400 K	1400 K	1600 K	1700 K	2200 K	2200 K
N	128	128	1024	128	128	128	128
Density ^(a)	0.917	0.86	0.86	0.84	0.83	0.887	0.823
Q_4 -local	0.174	0.165	0.169	0.175	0.178	0.174	0.162
Q_6 -local	0.478	0.382	0.379	0.373	0.370	0.478	0.382
W_4 -local	-0.099	-0.015	-0.016	-0.014	-0.013	-0.099	-0.016
W_6 -local	-0.013	-0.046	-0.044	-0.042	-0.040	-0.013	-0.045
C_{QW} ^(b)		-0.55	-0.53	-0.53	-0.51		-0.54

^(a) Density relative to the crystal at 0 K.

^(b) Correlation coefficient for fluctuations in Q_6 and W_6 .

Comparing the values of the local order parameters in the solid and liquid runs at 1400 K, we see that the local order in the liquid remains quite high. There is a small decrease in the value of Q_4 and a 20% decrease in Q_6 on going from the crystal to the liquid. The percentage changes in the third-order invariants are larger, with the magnitude of W_4 decreasing by a factor of six, while the magnitude of W_6 increases by a factor of three. The value of W_6 in the liquid is remarkable in that it is larger in magnitude than the value for any of the space filling lattices (see table 2). This observation gives a clue to the nature of the local structure, namely that icosahedral geometry is favoured locally. In this geometry (see table 2) both Q_4 and W_4 are zero, while W_6 is large and negative. The decrease the magnitudes of Q_4 and W_4 combined with the increase in the magnitude of W_6 is consistent with a certain amount of local icosahedral order. Further evidence to support this hypothesis arises from the fluctuations. The last column in the table gives the correlation coefficient between fluctuations in Q_6 and W_6 . In the liquid state these fluctuations are strongly correlated, while the correlation coefficients of all other pairs of fluctuations are small (less than 0.1). Local fluctuations to h.c.p. or f.c.c. order would show strong correlations between Q_6 and W_4 with positive and negative signs respectively.

There are small changes in the local order parameters as the temperature is raised. Although one would expect all the order parameters to decrease in magnitude, Q_4 increases by a small amount as the temperature is raised from 1400 K to 1700 K, suggesting that there is less icosahedral and more f.c.c. order at the higher temperatures.

4. Discussion and conclusions

In order for the results from a small system to be extrapolated to the thermodynamic limit using the arguments in section 2.1. two conditions must be satisfied. First, the ratio of the curvature of the wells should remain constant, and secondly the difference in the values of $F(Q_i)$ and $F(Q_c)$ should not change as the system size is increased. The first condition need not be stringently satisfied as the ratio of the curvatures only enters logarithmically. There is no obvious reason for a large change in this quantity. The definition of the Landau free energy in equation (4) shows that it depends on the logarithm of the integral of $\exp(-\beta H_0 + p_{\text{ext}} V)$ over a constant Q surface in the phase space of the system. Provided the system is large enough that the properties of the homogeneous bulk phases are not significantly distorted by the periodic boundaries, F is extensive (in the thermodynamic sense) and the Landau free energy per particle is unchanged as the system size increases. Comparison of the local order parameters in runs with 128 and 1024 particles (see table 3) shows that the local properties are very similar in the two runs, giving us confidence that the 128 particle runs are big enough for the determination of the relative free energy minima corresponding to the bulk homogeneous phases.

The interpretation of the free energy barrier in the small systems in terms of the surface free energy between the phases is, however, suspect, as the number of atoms in the surface region is comparable to the numbers in the bulk. Indeed it is difficult to see regions of order and disorder in snapshots of the small systems. The 1024 particle simulation, on the other hand, is big enough to allow one to estimate the surface free energy, without being too big to find a smooth transition from spherical to cylindrical or slab geometry.

It is interesting that the potentials used in this work should behave so differently

from the soft sphere potential used in earlier work. The latter is shorter-ranged and purely repulsive, which might explain why the more open b.c.c. structure seems to be favoured in the freezing soft sphere liquid. Alexander and McTague [17] gave general symmetry arguments that suggest that icosahedral or b.c.c. structures should form preferentially near the freezing transition. In this material we have evidence for local icosahedral order rather than b.c.c. order. As icosahedra are not space filling this preferred order cannot nucleate a solid phase. In the soft sphere liquid local b.c.c. order is found which can and does nucleate a solid phase. Alexander and McTague emphasize that their theory should apply to weakly first-order transitions. The values of $\Delta H_{\text{fus}}/kT_m$ for the potentials used in this work are 1.22 (Pt) and 1.3 (Rh) [10]. Further work on the relation of nucleation of solid phases of different structures, the local structure in the liquid phase, and the form of the potential is clearly indicated.

In summary, this work clearly demonstrates the difference between the thermodynamic melting point and the limit of metastability of a solid. The method of van Duijneveldt and Frenkel can be used to measure the difference in free energy between two phases more easily and as accurately as by other simulation techniques. In addition one may obtain information about the free energy of the surface between the phases and about mechanisms of nucleation of the solid phase.

R.M.L.B. thanks the FOM institute for hospitality when this work was started and J. Klinowski and D. Cvijovic for information about the plumber's nightmare triply periodic surfaces. Financial support was given by SERC for computing equipment (grant GR/HO4190). The work of the FOM Institute is part of the research program of FOM and is supported by the 'Nederlandse Organisatie voor Wetenschappelijk Onderzoek' (NWO).

References

- [1] PHILLPOT, S. R., LUTSKO, J. F., WOLF, D., and YIP, S., 1989, *Phys. Rev. B*, **40**, 2831.
- [2] LUTSKO, J. F., WOLF, D., PHILLPOT, S. R., and YIP, S., 1989, *Phys. Rev. B*, **40**, 2841.
- [3] SWOPE, W. C., and ANDERSEN, H. C., 1990, *Phys. Rev. B*, **41**, 7042.
- [4] VAN DUINEVELDT, J., and FRENKEL, D., 1992, *J. chem. Phys.*, **96**, 4655.
- [5] SUTTON, A. P., and CHEN, J., 1990, *Phil. Mag. Lett.*, **61**, 139.
- [6] FINNIS, M. W., and SINCLAIR, J. E., 1984, *Phil. Mag. A*, **50**, 45.
- [7] TORREY, G. M., and VALLEAU, J. P., 1974, *Chem. Phys. Lett.*, **28**, 578.
- [8] LANDAU, L. D., and LIFSHITZ, E. M., 1980, *Statistical Physics* (Oxford: Pergamon).
- [9] STEINHARDT, P. J., NELSON, D. R., and RONCHETTI, M., 1983, *Phys. Rev. B*, **281**, 784.
- [10] TODD, B. D., and LYNDEN-BELL, R. M., 1993, *Surf. Sci.*, **281**, 191.
- [11] LYNDEN-BELL, R. M., 1992, unpublished calculations.
- [12] KLINOWSKI, J., and CVIJOVIC, D., 1992, private communication.
- [13] MIEDEMA, A. R., 1978, *Z. Metallk.*, **69**, 287.
- [14] MIEDEMA, A. R., and DEN BROEDER, F. J. A., 1979, *Z. Metallk.*, **70**, 14.
- [15] MIEDEMA, A. R., and BOOM, R., 1978, *Z Metallk.*, **69**, 183.
- [16] STRICKLAND-CONSTABLE, R. F., 1968, *Kinetics and Mechanism of Melting* (London: Academic), p. 97.
- [17] ALEXANDER, S., and MCTAGUE, J., 1978, *Phys. Rev. Lett.*, **41**, 702.
- [18] MACMILLAN, N. H., and KELLY, A., 1972, *Proc. Roy. Soc. A*, **330**, 291.